Pressure induced state in the orthorhombic $(Mn_{1-x}Co_x)_2P$ system

2008 J. Phys.: Condens. Matter 20 195207

(http://iopscience.iop.org/0953-8984/20/19/195207)

J. Phys.: Condens. Matter **20** (2008) 195207 (7pp) doi:10.1088/0953-8984/20/19/195207

Pressure induced state in the orthorhombic $(Mn_{1-x}Co_x)_2P$ system

R Zach[1,5], Y Fukami[2], J Toboła[3], F Ono[2] and D Fruchart[4]

[1] Institute of Physics, Faculty of Physics, Mathematics and Applied Computer Science, Cracow University of Technology, Podchorążych, 1, 30-084 Cracow, Poland
[2] Science Department, Okayama University, Tsushima Naka, Okayama, Japan
[3] Faculty of Physics and Applied Computer Science, AGH University of Science and Technology, Aleja Mickiewicza 30, 30-059 Cracow, Poland
[4] Department MCMF, Institute Néel, CNRS, BP 166X, 38042 Grenoble cedex 9, France

E-mail: puzach@cyfronet.krakow.pl

Received 23 December 2007, in final form 12 March 2008
Published 11 April 2008
Online at stacks.iop.org/JPhysCM/20/195207

Abstract

In this paper we present the results of ac susceptibility measurements of a $(Mn_{0.65}Co_{0.35})_2P$ sample under pressure up to 7.5 GPa. The pressure induced low temperature ferromagnetic state in pressures above 5–6 GPa was established. Theoretical analysis of the electronic band structure 'under pressure' was carried out by the Korringa–Kohn–Rostoker method incorporating the coherent potential approximation (KKR-CPA). We could conclude that the local magnetic moment decreases with pressure. Moreover, when external pressure is applied along the *c*-axis, in the case of manganese atoms placed at the tetrahedral site, the magnetic moment practically disappears, but in the case of Co decreases only slightly. This type of behavior may be responsible for the pressure induced phase transition from the antiferromagnetic (AF) state to the ferromagnetic (F) state. KKR-CPA electronic band structure calculations undertaken in the antiferromagnetic state are also presented from which it was found that the density of states (DOS) at the Fermi level varies with applied pressure in the opposite way, when accounting for F and AF states. The rapid decrease of DOS at E_F in the ferromagnetic $(Mn_{0.65}Co_{0.35})_2P$ additionally supports the experimentally observed pressure induced AF–F transition.

(Some figures in this article are in colour only in the electronic version)

1. Introduction

The $(Mn_{1-x}Co_x)_2P$ system crystallizes in an orthorhombic crystal structure of Co_2P type (SG: *Pnma*) over a wide composition range $0.2 < x < 1$ (figure 1). However, for $x < 0.2$ the hexagonal Fe_2P type (SG: $P\bar{6}2m$) crystal structure is retained. In the range $0 < x < 0.5$, manganese substitutes on the pyramidal sites only, while for higher Mn contents i.e. $x > 0.5$, it substitutes on a tetrahedral site.

The Curie temperature and total magnetization are strongly sensitive to composition and exhibit a sharp maximum for MnCoP ($T_C = 570$ K, $M_{tot} = 3.2\ \mu_B$) [1]. Both these parameters markedly decrease when the Mn content increases. Compounds with $x > 0.4$ all exhibit ferromagnetic (F) properties, then metamagnetic behavior was observed for Mn contents $0.2 < x < 0.4$. At low temperature and for this composition range, a rather complex magnetic phase diagram was established [1–7].

Neutron diffraction studies on powder samples of MnCoP have been performed by several groups [1–5], and they showed that magnetic structure is mostly of ferromagnetic type with, however, more complex behavior at low temperatures. The values of magnetic moments ($T = 77$ K) for Mn and Co were estimated as 2.55 and 0.65 μ_B, respectively [6, 7].

Calculated values of the magnetic moments $\mu_{tot} = 3.03\ \mu_B$/f.u. for MnCoP were established and good agreement with the experimental values was found. Moreover, the change of the density of states (DOS) near the Fermi level from MnFeP to MnCoP tentatively explained the mechanism for the AF–F magnetic transition as detected experimentally in the

[5] Author to whom any correspondence should be addressed.

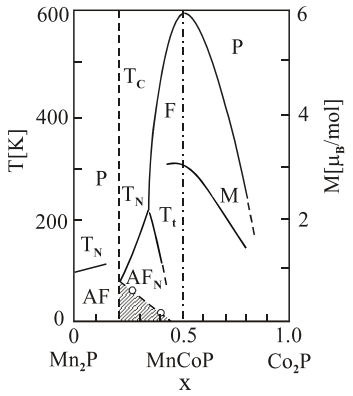

Figure 1. (x, T) magnetic phase diagram $(Mn_{1-x}Co_x)_2P$. AF, F, P, AF_N denotes antiferromagnetic, ferromagnetic, paramagnetic, and noncollinear antiferromagnetic phases, respectively. T_N: the Néel temperature, T_C: the Curie temperature, T_t : AF_N–F phase transition temperature, M: magnetization. The shaded area represents different types of AF_N structure [1].

investigated systems. Recently a detailed analysis of MnCoP electronic band structure was presented in the papers [8, 9].

As was mentioned above, in the orthorhombic crystal structure domain of the $(Mn_{1-x}Co_x)_2P$ series of compounds two magnetic phase transitions were found (see the (x, T) magnetic phase diagram, figure 1) the first one between noncollinear antiferromagnetic (AF_N) and F states (at T_t) and the second one between a ferromagnetic and a paramagnetic state (at T_C). The sample with $x = 0.35$ was chosen for ac susceptibility measurements under pressure. Two pressure ranges were chosen for high pressure analysis. Firstly, the low pressure data collected up to 1.5 GPa in the temperature range 80–420 K have already been presented [7, 8, 10]. Secondly, the ac susceptibility measured in the course of this work, up to 8 GPa in the temperature range 4.2–420 K will be analyzed in this paper.

The (P, T) magnetic phase diagram for the $(Mn_{1-x}Co_x)_2P$ with $x = 0.35$ sample was prepared on the basis of the temperature dependence of ac susceptibility under constant pressure [8, 10]. For $x = 0.35$ the T_C slope versus pressure is positive ($dT_C/dP = 10.6 \pm 1.2$ K GPa^{-1}) while T_t decreases with pressure ($dT_t/dP = -26.9 \pm 0.6$ K GPa^{-1}). Moreover, the pressure dependence of the critical field for the $(Mn_{0.65}Co_{0.35})_2P$ samples was studied at 78 K in pulsed magnetic field. The critical field value of B_C decreases with pressure and dB_C/dP is equal to $-0.18(6)$ T GPa^{-1} for $(Mn_{0.65}Co_{0.35})_2P$ [10, 13]. It is worthwhile noting that the field induced phase transitions found in the pressure magnetization measurements were also confirmed by magnetization measurements in continuous dc magnetic field carried out under atmospheric pressure.

Summarizing the ac susceptibility and pulsed field magnetization experiments carried out for $(Mn_{1-x}Co_x)_2P$ under pressure (up to 1.5 GPa) we may conclude that such behavior suggests that the ferromagnetic phase is stabilized with increasing pressure. It is worth noting that magnetization measurements remain in good agreement with the ac susceptibility measurements.

Table 1. Lattice parameters a, b, c and unit cell volume V refined at 100 K and 300 K for $(Mn_{0.65}Co_{0.35})_2P$ [8].

Lattice and atomic position parameters	100 K (AF_N)		300 K (F)	
a (10^{-10} m)	5.9489(7)		5.9569(8)	
b (10^{-10} m)	3.5342(4)		3.5460(5)	
c (10^{-10} m)	6.7426(5)		6.7622(1)	
V (10^{-30} m^3)	141.76(3)		142.84(4)	
$x_{(Mn,Co)}$, $z_{(Mn,Co)}$	0.868(4)	0.064(2)	0.845(4)	0.041(3)
x_{Mn}, z_{Mn}	0.960(2)	0.659(2)	0.968(2)	0.635(2)
x_P, z_P	0.266(4)	0.104(3)	0.185(3)	0.126(4)

The linear dependence of critical field B_C versus pressure P leads us to a conclusion that the low temperature antiferromagnetic AF_N phase observed under atmospheric pressure may be replaced in the higher pressure range by a new pressure induced ferromagnetic state. So the aim of this paper is to confirm (or to deny) the existence of the high pressure induced state in the pressure range up to 8 GPa. It is worth noting that, until now, Curie temperature measurements under high pressure had only been carried out by Nakagiri *et al* [11].

2. Experimental study

2.1. Sample synthesis

Polycrystalline samples were synthesized starting from the appropriate proportion of 99.99% pure elements. The fine powders of the elements were mixed then progressively heated up to 850 °C for 10 days in evacuated silica tubes. The final heat treatment performed by high frequency heating allowed melting of the sample before cooling it down to room temperature [1, 2]. The quality of the samples was verified both by x-ray diffraction analysis as well as by magnetization measurements in weak magnetic field. X-ray diffraction experiments for the studied sample were performed using a Philips diffractometer, with Bragg–Brentano geometry. No extra parasite phases or pure elements as impurities in the spectra were found. Our refinements showed that the studied content was the fully stoichiometric compound. Lattice parameters determined at room temperature remain in good agreement with those previously reported [1, 8] (see table 1).

2.2. ac susceptibility measurements under high pressure

A cubic anvil press was used for ac susceptibility measurements under pressure up to 7.5 GPa [12]. Powdered samples were put into a cylinder with radius 0.7 mm and a length of 1.5 mm beforehand. To detect the ac susceptibility signal, primary and secondary coils were wound around the sample. The sample and the coil system were inserted, with a liquid pressure medium, fluorinert, into a Teflon capsule (inner diameter 1.6 mm and length 1.7 mm). Then this capsule was set in the center of the cubic cell made of pyrofillate, which was compressed uniformly by six tungsten carbide (WC) anvils with edge length 4 mm. Temperature was measured by a silicon diode (4.2–400 K). The ac magnetic field was generated by the

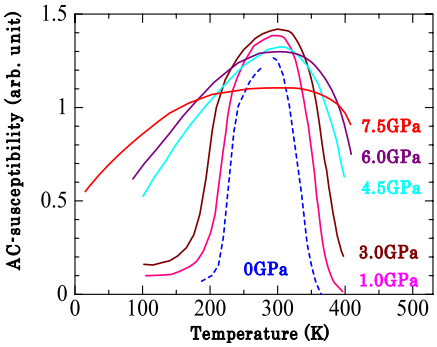

Figure 2. Ac susceptibility curves versus temperature measured for $(Mn_{0.65}Co_{0.35})_2P$ at different pressures up to 7.5 GPa [13].

primary coil and the signal induced in the secondary coil was measured by the lock-in nanovoltmeter. The frequency of the maximum magnitude was 990 Hz. By using the present high pressure equipment a maximum pressure of 7.5 GPa was generated in a hydrostatic condition. The quality of the hydrostatic condition of the present system was proved to be so good as to preserve the life of a tiny animal, tardigrade [18], up to the maximum pressure of 7.5 GPa. However, it should be mentioned here that the fluorinert (FC70) was used as a pressure transmitting medium and the hydrostatic pressure limit of different kinds of the fluorinert has been recently presented [19]. Because of the fact that the fluorinert freezes at a higher pressure range a deviatoric stress state to the sample may be also provided (∼3.2 GPa) [20].

3. Results and discussion

3.1. Ac susceptibility studies under high pressure

Ac susceptibility measurements of the $(Mn_{0.65}Co_{0.35})_2P$ composition (the orthorhombic crystal structure domain) under pressure up to 8 GPa (cubic anvil press) were undertaken in the course of this work. The ac susceptibility of $(Mn_{0.65}Co_{0.35})_2P$ versus temperature measured at different pressures up to 7.5 GPa are presented in figure 2. The ac susceptibility curve obtained in the atmospheric pressure shows a broad maximum corresponding to the temperature region in which the ferromagnetic phase exists. The antiferromagnetic and paramagnetic phases are confirmed at low and high temperatures, respectively.

The temperature dependence of ac susceptibility at pressures $P = 1.0$ and 3.0 GPa is very similar to that measured at atmospheric pressure. The isobaric ac susceptibility curves obtained for $(Mn_{0.65}Co_{0.35})_2P$ at different pressures allow us to conclude that the Curie temperature increases versus pressure ($dT_C/dP = 10$ K GPa^{-1}), at least up to 3 GPa, however, the temperature T_t decreases with pressure ($dT_t/dP = -28$ K GPa^{-1}). Furthermore, the temperature range ΔT, where the ferromagnetic phase is stable, changes slightly when an external pressure is applied. For instance, the calculated ΔT values (as large as ∼120 and ∼220 K at atmospheric and 3 GPa pressures, respectively) suggest that the ferromagnetic state becomes more stable at higher pressures. Moreover, the shape of the ac susceptibility curves measured in the low temperature range (i.e. below 200 K), shows the evidence that in this temperature range the AF_N noncollinear antiferromagnetic state exists below ∼175 K and under a pressure of 3 GPa.

The analysis of the ac susceptibility evolution at 4.5 GPa and 6 GPa leads to the following conclusions: the Curie temperature increases with pressure, as was the case for the samples reported above, the temperature range ΔT, where the ferromagnetic phase is stable, increases versus pressure, and at 6 GPa the ΔT value is greater than 350 K but no antiferromagnetic states exist about 100 K.

The temperature dependence of the ac susceptibility measured at the highest pressure produced by our cubic anvil press, i.e. at 7.5 GPa, is presented in figure 2. It can be seen that the ac susceptibility at 200 K is twice as much as at 4.2 K. Furthermore, the highest recorded value of the susceptibility remains practically constant up to 350 K. Above this temperature a steep descent of the ac susceptibility, associated with the Curie temperature, is observed. It seems reasonable to assume that for $(Mn_{0.65}Co_{0.35})_2P$ at 7.5 GPa the pressure induced ferromagnetic state was established in a wide temperature range.

To summarize the above ac susceptibility behavior under high pressure it may be concluded that [13]:

(i) the Curie temperature increases with pressure;
(ii) the AF_N–F phase transition temperature T_t strongly decreases with pressure;
(iii) the pressure induced ferromagnetic state was established at low temperatures (4.2–80 K) and at 6–8 GPa pressure range.

3.2. Theoretical study

The effect of hydrostatic pressure on the electronic structure and magnetic properties in the orthorhombic $(Mn_{0.65}Co_{0.35})_2P$ have been simulated by compressing the unit volume cell ($\Delta V/V$ up to about 5%) through a selective decrease of lattice constants. To simplify the analysis, the relative atomic positions in the unit cell were kept unchanged (table 1). At the first step, the ferromagnetic state of $(Mn_{0.65}Co_{0.35})_2P$ was assumed in the calculations. For the c-axis compression, where the modifications of electronic states close to the Fermi level appeared to be the most noticeable, electronic structure computations have also been performed assuming the antiferromagnetic state. Since the low temperature antiferromagnetic structure [6] of $(Mn_{1-x}Co_x)_2P$ with $x = 0.6$ and 0.75 is rather complex due to incommensurate magnetic ordering, suggesting a 'double-helix' type of magnetic structure, the collinear approximation has been used with the AF cell corresponding to the c-axis doubled chemical cell. Notably, in our previous study, different types of AF ordering in the isostructural $MnFe_{1-x}Co_xP$ system were considered [9]. It was concluded that AF coupling between larger Mn magnetic moments (the pyramidal site) plays a predominant role in lowering both DOS at E_F as well as the total energy of the system. In the case of $(Mn_{0.35}Co_{0.65})_2P$, we have followed the aforementioned result in order to select the

Table 2. Illustrative results of electronic structure KKR-CPA calculations 'under pressure' for $(Mn_{0.65}Co_{0.35})_2P$ [13]. The values of the magnetic moments of Mn, Co, and P atoms distributed in pyramidal and/or tetrahedral sites are presented (as well as total magnetic moment, M_{TOT}) for two unit cell compressions ($\Delta V/V = 2.5$ and 5%) both in ferromagnetic (F) and antiferromagnetic (AF) states (see also figure 3).

Pressure/ ordering	M_{TOT} (μ_B)	Mn_T (μ_B)	Co_T (μ_B)	Mn_P (μ_B)	P (μ_B)
			$\Delta V/V = 0\%$		
Normal, F	11.10	0.22	0.27	2.63	−0.05
			$\Delta V/V = 2.5\%$		
c-axis, F	10.47	0.06	0.26	2.51	−0.04
c-axis, AF	0.0	0.16	0.22	2.52	−0.02
			$\Delta V/V = 5\%$		
a-axis, F	10.21	0.13	0.28	2.42	−0.05
b-axis, F	9.86	−0.05	0.27	2.39	−0.04
c-axis, F	9.74	−0.03	0.28	2.34	−0.03

most plausible collinear approximations. In the AF structure, the neighboring [0, 1/4, 0] and [0, −1/4, 0] planes of the Mn magnetic moments (pyramidal site) were coupled AF (the 'inter' coupling), whereas the Mn moments were aligned as either F or AF within each plane (the 'intra' coupling). More details describing the considered magnetic structure can be found in [9]. The aforementioned AF model appears to be a reliable collinear approximation of the experimentally observed magnetic ordering at low temperature.

Computations of $(Mn_{0.65}Co_{0.35})_2P$ in the AF state were performed in the case of *c*-axis compression only, since they are complicated due to the disordered effects accounting for two tetrahedral sites ($c' = 2c$) as well as the low symmetry of the unit cell. However, we suppose that the external pressure influences mostly the *c*-axis, as has already been observed in similar series of compounds (e.g. $MnRh_{1-x}Co_xAs$ and $MnRhAs_{1-x}P_x$ [16]) and is supported by our theoretical results in the ferromagnetic state.

Electronic structure computations of $(Mn_{0.65}Co_{0.35})_2P$ have been performed using Korringa–Kohn–Rostoker method incorporating the coherent potential approximation (KKR-CPA) [14, 15], being adapted to chemically disordered systems. Crystal potentials of muffin-tin form have been constructed within the local-spin density framework (LSD), using the von Barth–Hedin expression for the exchange–correlation potential [17]. For well-converged charges and potentials the total site-decomposed and l-decomposed spin-polarized DOS were calculated, as well as total and local magnetic moments around inequivalent atoms. The lattice constants had reduced successively by about 2.5 and 5%, which well reflects the physically penetrable range of the volume decrease with the applied pressure (up to ∼8 GPa). In the case of $MnRhAs_{0.6}P_{0.4}$, which is a similar compound, ∼3 $Å^3$/f.u. decrease of volume was found when $P = 10$ GPa [16].

3.3. F and AF states 'under pressure'

Figure 3 presents the DOS in ferromagnetic $(Mn_{0.65}Co_{0.35})_2P$ when compressing selectively *a*-, *b*-, and *c*-axes of the orthorhombic unit cell. In each case the lattice constant was decreased in order to obtain the same volume change (<5%). A detailed analysis of the electronic structure of the ferromagnetic $(Mn_{1-x}Co_x)_2P$ system (at normal pressure) has already been reported in [8, 10]. We can only recall that the MnCoP compound exhibits a very low DOS at E_F for both spin directions and it rapidly increases when substituting Co with Mn on the tetrahedral site. This was concluded to be a tentative origin of the F–AF transition in samples richer in Mn. The presence of such a deep valley of DOS behavior can also be found in $(Mn_{0.65}Co_{0.35})_2P$ (figure 3) but just above the Fermi level. In comparison to MnCoP, E_F is shifted down more or less in a rigid way to the region of high DOS both for up- and down-spin electrons, due to the decreased number of electrons in the system (figures 4 and 5).

The effect of the 'pressure' on electronic states near E_F can be clearly seen, when inspecting the case of the *c*-axis contraction. The decreasing spin-polarization of total electronic states in $(Mn_{0.65}Co_{0.35})_2P$ is mainly due to an important decrease in the Mn magnetic moment on the pyramidal site (table 2). The other effect of the pressure corresponds to the broadening of the conduction band, when the interatomic distances decrease. However, the most attractive behavior upon pressure being applied is related to the particular character of the spin-polarized DOS, which appears to be similar to a 'half-metallic' ferromagnetic state. The developing of a pseudo-gap for spin-down electrons is especially well seen in the case of the *c*-axis compression (the spin-up DOS is not visibly modified). The volume cell shrinking of the ferromagnetic $(Mn_{0.65}Co_{0.35})_2P$ results in a rapid decrease of the total DOS at E_F (figure 4). Such an electronic structure feature also yields an important decrease of the total energy of the system (particularly for the compression along the *a*- and *c*-axes). The comparison of the total energy of the ferromagnetic $(Mn_{0.65}Co_{0.35})_2P$ for 'normal' (at ambient pressure) and axially pressed samples supports the DOS modifications. It appears that the *a*- and *c*-axis compression is energetically favorable for the system, while decreasing the volume along the *b*-axis is not beneficial.

The effect of *c*-axis 'pressure' on DOS near E_F was also studied in the AF $(Mn_{0.65}Co_{0.35})_2P$ compound (figure 5(b)). The most striking difference between two types of magnetic ordering (F versus AF) is related to the DOS variations near

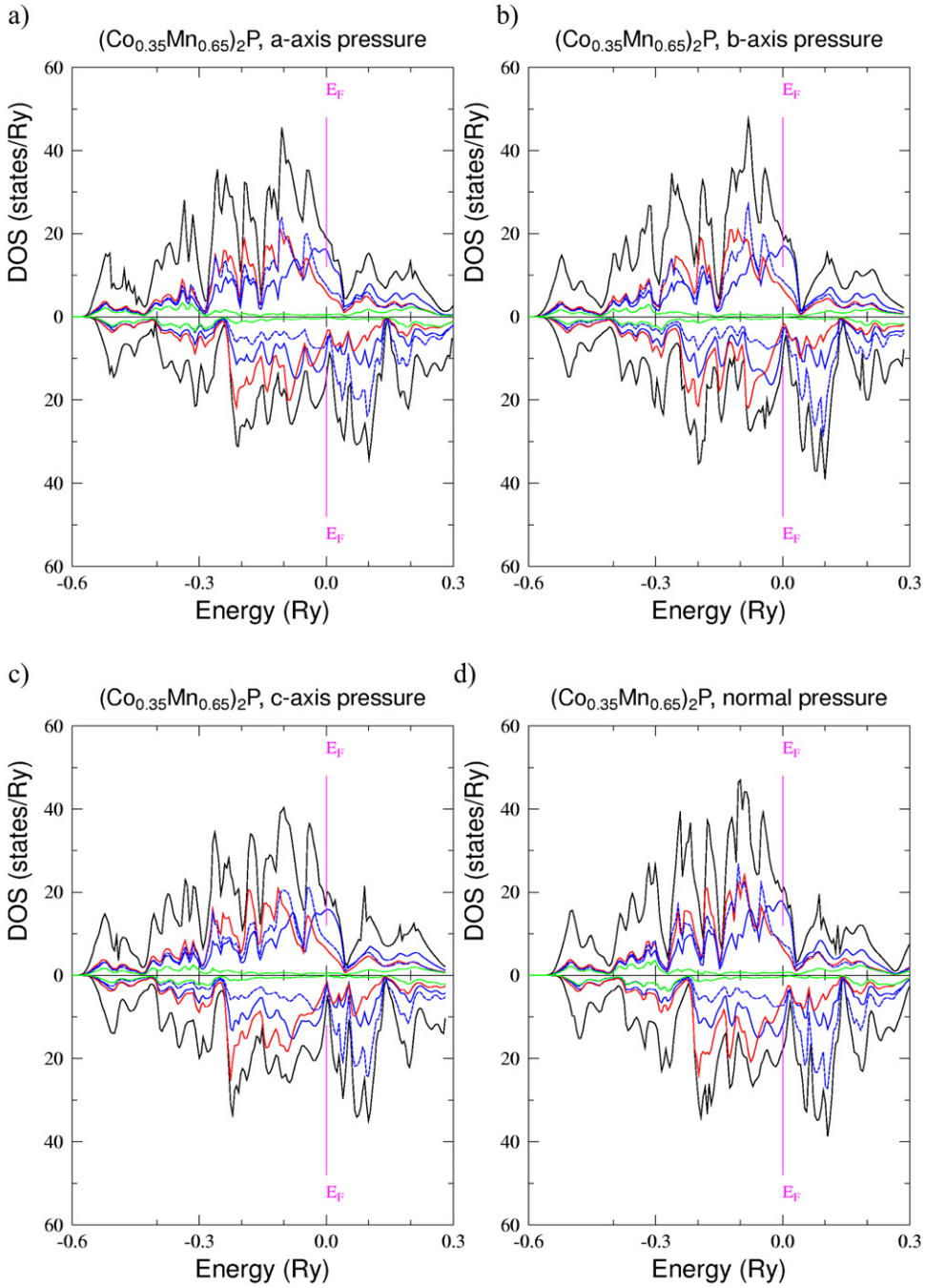

Figure 3. Total and site-decomposed DOS: Co (red, online), Mn (blue, online), tetrahedral (solid) and pyramidal (dashed) site, *a*-axis, *b*-axis, and *c*-axis represent the compression of the lattice along *a*, *b*, and *c* axes, respectively [13], whereas 'normal' denotes the ambient pressure conditions.

E_F with decreasing volume (figure 5). $N(E_F)$ smoothly increases with *c*-axis pressure in the AF state, whereas it decreases more rapidly in the F one. In view of the $N(E_F)$ criterion, the ferromagnetic state tends to be more stable than the antiferromagnetic one, for the relative volume compression $(\Delta V/V)$ becoming larger than ∼1%. The KKR-CPA results well support the experimental observation of the pressure induced AF–F transition observed in $(Mn_{0.65}Co_{0.35})_2P$. This behavior seems to be in line with high pressure measurements in the range where non-hydrostatic conditions probably appear. Such a situation could favor directional stresses experienced by the sample. Our theoretical results support the experimental findings, showing evidence of an increasing temperature interval of the ferromagnetic domain in the high pressure range.

4. Conclusions

For the $(Mn_{0.65}Co_{0.35})_2P$ sample in the pressure range 6–8 GPa *a pressure induced ferromagnetic state* was found at low temperatures (4.2–80 K). Band structure calculations 'under pressure' were carried out with the assumption that the relative

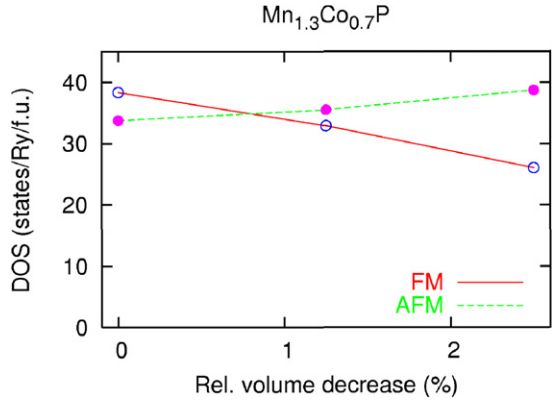

Figure 4. Variation of total DOS at E_F in ferromagnetic (F) and antiferromagnetic (AF) $(Mn_{0.65}Co_{0.35})_2P$ with decreasing relative volume of the unit cell ($\Delta V/V$ given in %). The lines connecting computed points are given as a guide to the eye.

change of the unit cell volume $\Delta V/V < 5\%$. The following conclusions can be drawn (figure 3, table 2).

(i) The DOS at the Fermi level decreases with pressure applied along any axis. The highest decrease of DOS was found in the case of *c*-axis applied pressure. Moreover, for the spin-down sub-band the pseudo-gap behavior was developed for spin-down electrons, suggesting a tendency to 'half-metallic ferromagnetism'.

(ii) The computed local magnetic moments in $(Mn_{0.65}Co_{0.35})_2P$ decrease versus pressure (particularly for the large moment on the pyramidal Mn atoms) and are comparable in F and AF states.

(iii) The magnetic moments on Mn atoms on tetrahedral sites are very sensitive to the volume decrease and practically disappear with the *c*-axis compression, whereas they decrease only slightly on Co atoms. This type of behavior may be responsible for the pressure induced AF–F phase transition.

(iv) For *c*-axis compression in $(Mn_{0.65}Co_{0.35})_2P$, the total DOS at the Fermi level behaves in the opposite way, i.e. it rapidly decreases in the F state, whereas it slightly increases in the AF state. This result agrees well with the development of the F coupling between the transition metal atoms with external pressure (against the AF coupling), as observed from the ac susceptibility curves.

Finally, it should be summarized that the observed increase of the ferromagnetic interactions in the $(Mn_{1-x}Co_x)_2P$ system in the orthorhombic crystal structure domain may be caused by external applied pressure, and/or by increasing the cobalt content in the studied series of solid solutions [10].

Acknowledgment

Financial support from the Ministry of Science and Education through grant No. 1 P03B 113 29 is gratefully acknowledged (JT and RZ).

References

[1] Roger A 1970 *PhD Thesis* Universite de Paris
[2] Fruchart D, Martin-Farrugia C, Rouault A and Sénateur J P 1980 *Phys. Status Solidi* a **57** 675
[3] Radhakrishna P, Fujii H, Doniach S, Reichardt W and Charpin P 1987 *J. Magn. Magn. Mater.* **70** 229
[4] Radhakrishna P, Fujii H, Brown P J, Doniach S, Reichardt W and Schweiss P 1990 *J. Phys.: Condens. Matter* **2** 3359
[5] Fruchart D, Nizioł S, Chenevier B and Roudaut E 1985 *SCTE'85: 8th Int. Conf. on Solid Compounds of Transition Elements (Vienna)*
[6] Puertolas J A, Rillo C, Bartolome J, Fruchart D, Niziol S, Zach R and Fruchart R 1988 *J. Physique Coll.* **49** C8197
[7] Nizioł S, Zach R, Fruchart D, Bombik A, Pacyna A W and Fruchart R 1993 *J. Magn. Magn. Mater.* **127** 103
[8] Średniawa B, Zach R, Chajec W, Duraj R, Toboła J, Nizioł S, Kaprzyk S, Fruchart D and Bacmann M 2002 *J. Magn. Magn. Mater.* **242–245** 931
[9] Zach R, Toboła J, Średniawa B, Kaprzyk S, Guillot M, Fruchart D and Wolfers P 2007 *J. Phys.: Condens. Matter* **19** 376201
[10] Średniawa B 2003 *PhD Thesis* AGH, Kraków
[11] Nakagiri N, Yamamoto Y, Nomura M, Fujii H, Okamoto T and Fujiwara H 1983 *J. Phys. Soc. Japan* **52** 246
[12] Mori N, Takahashi H and Miyane Y 1990 *Solid State Phys.* **25** 185
[13] Zach R, Fukami Y, Sun N Q, Ono F, Toboła J and Fruchart D 2006 *SCTE'06: Int. Conf. on Solid Compounds of Transition Elements (Kraków, July)*

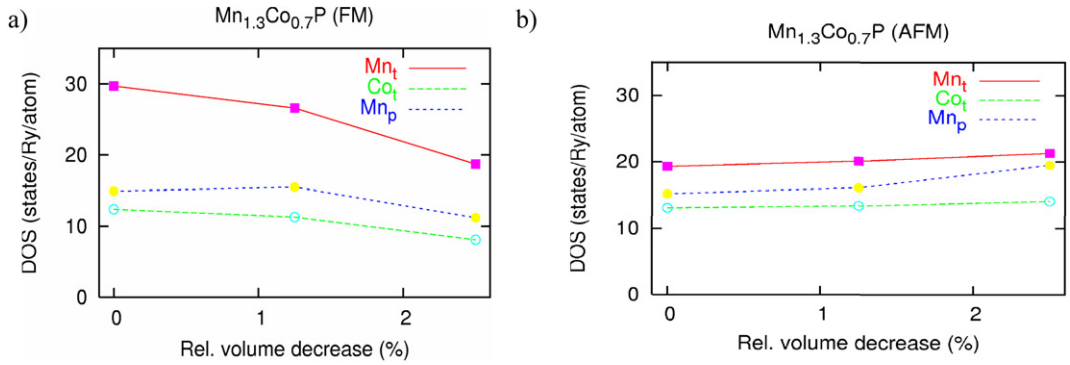

Figure 5. Variation of site-dependent DOS at E_F in F (left panel (a)) and AF (right panel (b)) $(Mn_{0.65}Co_{0.35})_2P$ with decreasing relative volume of the unit cell ($\Delta V/V$ given in %). The transition metal contributions are plotted only, i.e. manganese on tetrahedral (Mn_t) and pyramidal (Mn_p) sites as well as cobalt (Co_t) on the tetrahedral site. The lines connecting computed points are given as a guide to the eye.

[14] Bansil A, Kaprzyk S, Mijnarends P E and Toboła J 1999 *Phys. Rev.* B **60** 13396
[15] Stopa T, Kaprzyk S and Tobola J 2004 *J. Phys.: Condens. Matter* **16** 4921
[16] Fujii N, Zach R, Kanomata T, Nishihara H, Ono F, Ishizuka M and Endo S 2002 *J. Alloys Compounds* **345** 59
[17] Barth von U and Hedin L 1972 *J. Phys. C: Solid State Phys.* **5** 1629
[18] Ono F, Saigusa M, Uozumi T, Matsushima Y, Ikeda H, Saini N L and Yamashita M J 2008 *SCTE2007 Conf. (Miami, April 2007)*; *Phys. Chem. Solids* at press
[19] Varga T, Wilkinson A P and Angel R J 2003 *Rev. Sci. Instrum.* **74** 4564
[20] Kagi H, Parise J B, Loveday J S, Kuribayashi T and Kudoh Y 2003 *Geophysical Research Abstracts* vol 5 (Strasbourg: European Geophysical Society) p 09805